IJC
International Journal of Cancer

A pilot precision medicine trial for children with diffuse intrinsic pontine glioma—PNOC003: A report from the Pacific Pediatric Neuro-Oncology Consortium

Sabine Mueller[1,2,3], Payal Jain[4], Winnie S. Liang[5], Lindsay Kilburn[6,7], Cassie Kline[1,3], Nalin Gupta[2,3], Eshini Panditharatna[7,8], Suresh N. Magge[9], Bo Zhang[4], Yuankun Zhu[4], John R. Crawford[10], Anu Banerjee[2,3], Kellie Nazemi[11], Roger J. Packer[7], Claudia K. Petritsch[2], Nathalene Truffaux[1], Alison Roos[5], Sara Nasser[5], Joanna J. Phillips[2,12], David Solomon[12], Annette Molinaro[2], Angela J. Waanders[4,13,14], Sara A. Byron[5], Michael E. Berens[5], John Kuhn[15], Javad Nazarian[4,6,7,8]*, Michael Prados[2]* and Adam C. Resnick[4,14,16]*

[1]Department of Neurology, University of California San Francisco, San Francisco, CA, USA
[2]Department of Neurological Surgery, University of California San Francisco, San Francisco, CA, USA
[3]Department of Pediatrics, University of California San Francisco, San Francisco, CA, USA
[4]Center for Data-Driven Discovery, Children's Hospital of Philadelphia, Philadelphia, PA, USA
[5]Translational Genomic Research Institute (TGEN), Phoenix, AZ, USA
[6]Center for Cancer and Blood Disorders, Children's National Health System, Washington, DC, USA
[7]Brain Tumor Institute, Children's National Health System, Washington, DC, USA
[8]Research Center for Genetic Medicine, Children's National Health System, Washington, DC, USA
[9]Division of Neurosurgery, Children's National Health System, Washington, DC, USA
[10]University of California San Diego, San Diego, CA, USA
[11]Doernbecher Children's Hospital, Oregon Health & Science University, Portland, OR, USA
[12]Department of Pathology, University of California San Francisco, San Francisco, CA, USA
[13]Department of Pediatrics, Perelman School of Medicine, University of Pennsylvania, Philadelphia, PA, USA
[14]Children's Brain Tumor Tissue Consortium, Children's Hospital of Philadelphia, Philadelphia, PA, USA
[15]College of Pharmacy, University of Texas Health Science Center, San Antonio, TX, USA
[16]Department of Biomedical and Health Informatics, Children's Hospital of Philadelphia, Philadelphia, PA, USA

This clinical trial evaluated whether whole exome sequencing (WES) and RNA sequencing (RNAseq) of paired normal and tumor tissues could be incorporated into a personalized treatment plan for newly diagnosed patients (<25 years of age) with diffuse

Key words: diffuse intrinsic pontine glioma, precision medicine, next generation sequencing, circulating tumor DNA, genomics-guided clinical trial

Abbreviations: CNS: central nervous system; CSF: cerebrospinal fluid; ctDNA: circulating tumor DNA; CLIA: clinical laboratory improvement amendments; CWL: common workflow language; CNAs: copy number alterations; CNV: copy number variation; DIPG: diffuse intrinsic pontine glioma; ddPCR: droplet digital polymerase chain reaction; FDA: food and drug administration; GEM: genomic-enabled medicine; H3K27M: histone 3 K27M mutation; HDAC: histone deacetylase; KMS: Kaplan–Meier survival; LCR: low-complexity regions; MRI: magnetic resonance imaging; MAF: mutation allele frequency; NIH: National Institutes of Health; QC: quality control; RIN: RNA integrity number; RNAseq: RNA sequencing; SV: structural variant; TGEN: Translational Genomic Research Institute; UCSF: University of California San Francisco; WES: whole exome sequencing; WGS: whole genome sequencing

Additional Supporting Information may be found in the online version of this article.

Conflict of interest: The authors have no conflict of interest to declare.

*J.N., M.P. and A.C.R. shared senior authorship

Grant sponsor: Dragon Master Foundation; **Grant sponsor:** Gabriella Kids First Data Resource Center; **Grant sponsor:** Goldwin foundation; **Grant sponsor:** Kaminsky Foundation; **Grant sponsor:** Kortney Rose Foundation; **Grant sponsor:** Matthew Larson Foundation for Pediatric Brain Tumors; **Grant sponsor:** Musella Foundation For Brain Tumor Research and Information; **Grant sponsor:** Piedmont Community Foundation; **Grant sponsor:** Project Open DIPG; **Grant sponsor:** Smashing Walnuts Foundation; **Grant sponsor:** TGEN Foundation; **Grant sponsor:** V Foundation for Cancer Research; **Grant sponsor:** Pediatric Brain Tumor Foundation (Asheville, NC); **Grant sponsor:** PNOC Foundation and Jennys Quest for Cure Foundation

DOI: 10.1002/ijc.32258

History: Received 12 Nov 2018; Accepted 15 Feb 2019; Online 12 Mar 2019.

Correspondence to: Sabine Mueller, MD PhD MAS, Department of Neurology, Neurosurgery and Pediatrics, University of California, Sandler Neuroscience Building, 675 Nelson Rising Lane, Room 402B, San Francisco, CA 94148, USA, Tel.: +1 415-502-7301, Fax: +1 415-502-7299, E-mail: sabine.mueller@ucsf.edu

intrinsic pontine glioma (DIPG). Additionally, whole genome sequencing (WGS) was compared to WES to determine if WGS would further inform treatment decisions, and whether circulating tumor DNA (ctDNA) could detect the H3K27M mutation to allow assessment of therapy response. Patients were selected across three Pacific Pediatric Neuro-Oncology Consortium member institutions between September 2014 and January 2016. WES and RNAseq were performed at diagnosis and recurrence when possible in a CLIA-certified laboratory. Patient-derived cell line development was attempted for each subject. Collection of blood for ctDNA was done prior to treatment and with each MRI. A specialized tumor board generated a treatment recommendation including up to four FDA-approved agents based upon the genomic alterations detected. A treatment plan was successfully issued within 21 business days from tissue collection for all 15 subjects, with 14 of the 15 subjects fulfilling the feasibility criteria. WGS results did not significantly deviate from WES-based therapy recommendations; however, WGS data provided further insight into tumor evolution and fidelity of patient-derived cell models. Detection of the *H3F3A* or *HIST1H3B* K27M (H3K27M) mutation using ctDNA was successful in 92% of H3K27M mutant cases. A personalized treatment recommendation for DIPG can be rendered within a multicenter setting using comprehensive next-generation sequencing technology in a clinically relevant timeframe.

What's new?

While children diagnosed with diffuse intrinsic pontine glioma (DIPG) continue to suffer dismal survival outcomes, progress in next-generation sequencing technologies have advanced the possibility of personalized therapeutic interventions. This prospective study demonstrates the feasibility of performing biopsies on patients with DIPG at diagnosis, applying approaches in next-generation sequencing to determine an individualized therapy plan in a clinically relevant timeframe. Analyses of cell lines derived from patient samples revealed key genomic alterations typical of DIPG, including mutations in *ACVR1*, *H3F3A*/*HIST1H3B*, *PIK3R1*, *PPM1D*, and *TP53*. The study further highlights the utility of circulating tumor DNA for detecting driver mutations in DIPG.

Introduction

Diffuse intrinsic pontine glioma (DIPG) arise in the brainstem and predominantly affect children, with less than 10% of patients surviving more than 2 years, despite decades of research.[1,2] Recent advances in molecular profiling of tumors through whole exome sequencing (WES) and RNA sequencing (RNAseq) support the development of personalized, genome-guided clinical trials that may foster the development of new therapeutic interventions for DIPG.[3–5]

Until recently, analyses of DIPG tissue were mainly limited to specimens obtained from postmortem examination because surgical biopsy was considered to be associated with high risks. However, using modern surgical techniques, biopsy at the time of diagnosis can be done with acceptable risks and has become more accepted in the last several years.[6,7] This change in clinical practice has resulted in a significant increase in the availability of DIPG-related molecular data. Detailed genomic studies reveal that despite a homogeneous clinical and radiographic presentation, DIPGs are molecularly heterogeneous with dysregulation of multiple pathways within individual tumors.[8] This suggests that a single-agent treatment approach will likely fail, that combination therapies should be investigated and that there is a need for precision medicine approaches.[9,10]

Within this PNOC003 pilot study, we assessed the feasibility of implementing such a precision medicine strategy as a multi-institutional trial for children with newly diagnosed DIPG. We also tested the feasibility of developing patient-derived cell lines and performing longitudinal profiling of tumors at recurrence and autopsy and of ctDNA isolated from plasma during the disease course, all of which was done with the intent to inform the next generation of clinical trials.

Materials and Methods

Study design and participants

PNOC003 (Trial registration: clinicaltrials.gov/NCT02274987) is a multi-institutional clinical trial using molecularly targeted therapy with up to four FDA-approved drugs based on genetic profiling of paired tumor/constitutional specimens with WES and tumor RNAseq in children with newly diagnosed DIPG. Patients were enrolled in the feasibility study between September 2014 and January 2016. All patients and legal guardians provided written consent and assent where appropriate. Participating sites in this feasibility study included the University of California, San Francisco, (San Francisco, CA); Children's National Health System (Washington, DC); and the University of California, San Diego (San Diego, CA). The Translational Genomic Research Institute (TGEN; Phoenix, AZ) performed WES and RNAseq in a Clinical Laboratory Improvement Amendments (CLIA) approved environment (Ashion Analytics, Phoenix, AZ). Key inclusion criteria included age between 3 and 25 years, new diagnosis of DIPG

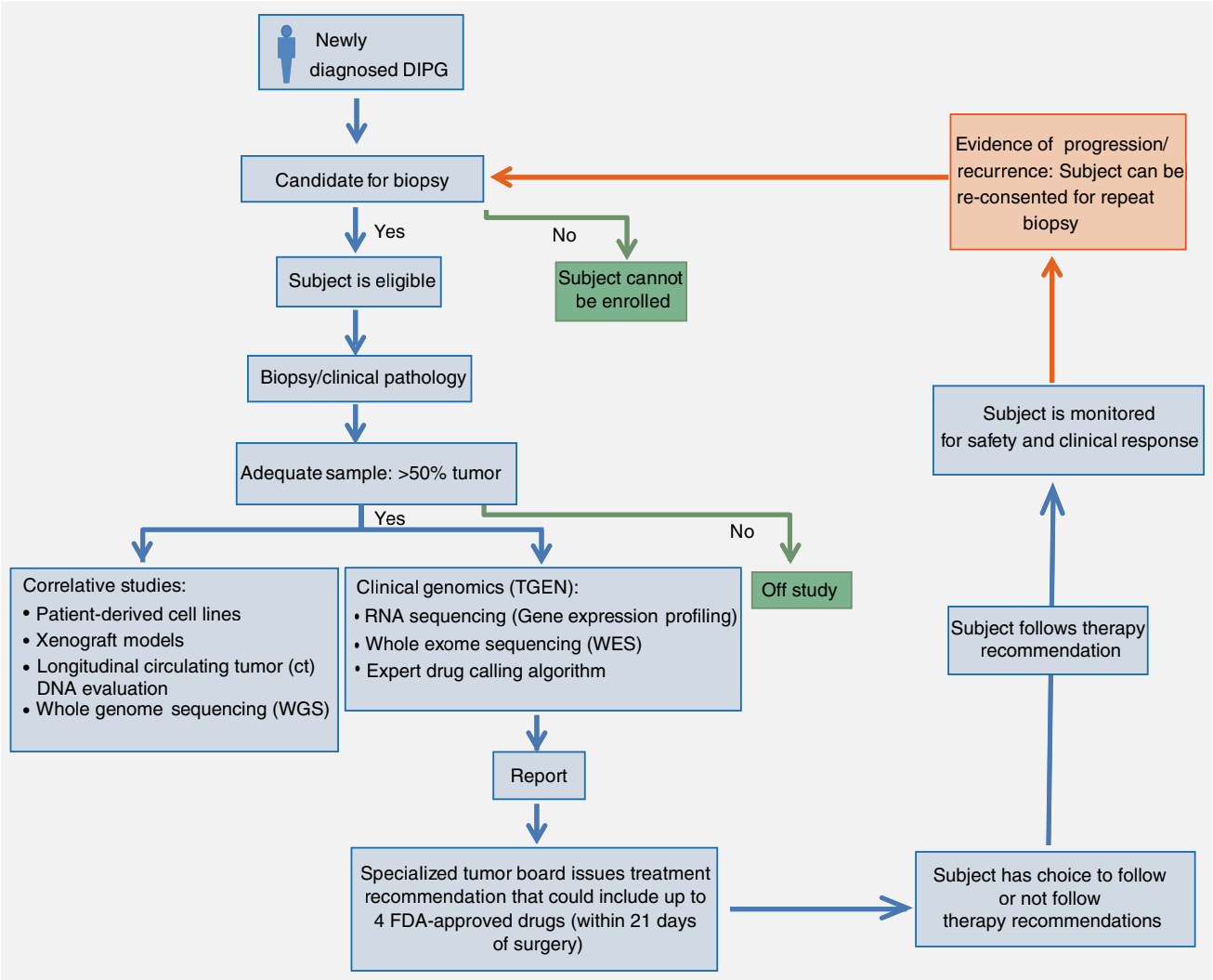

Figure 1. PNOC003 Feasibility Trial Design. Flow chart depicting PNOC003 feasibility trial design.

based upon clinical and radiographic findings with no evidence of dissemination (Fig. 1). Patients were enrolled prior to biopsy based on radiographic findings. Patients with pathology results not in support of DIPG diagnosis were subsequently excluded. Results of WES and RNAseq and drug-gene matching were presented by TGEN to a specialized tumor board consisting of a minimum of three pediatric neuro-oncologists and one dedicated neuro-pharmacologist (JK). Following treatment based on the tumor board treatment recommendation was optional. Every enrolled subject was followed for clinical and imaging endpoints as well as ctDNA collection until first progression. At the time of first progression, subjects had the option to undergo a repeat biopsy along with repeat WES and RNAseq analysis.

Sample collection and processing

Subjects underwent biopsies as part of standard clinical care at the participating clinical sites. Stereotactic needle biopsy was performed via a middle cerebellar peduncle approach, using frameless navigation. Standardization of surgical procedures at different centers was done by preenrollment training of participating neurosurgeons through the study neurosurgical chair (NG) as described previously.[6,11] A board-certified neuropathologist verified the diagnosis of a diffuse glial neoplasm and estimated tumor percentage. If tumor content was at least 50%, specimens were de-identified and sent to Ashion Analytics. If feasible, postmortem autopsy samples were also collected according to institutional protocols.[12]

Clinical reporting

Clinical data, including patient demographics, details surrounding the primary tumor (e.g., pathology diagnosis, results of laboratory testing), and additional relevant information such as concomitant medication use were entered into TGEN's clinical portal to generate a de-identified clinical report.

Clinical whole exome and transcriptome sequencing

WES of paired tumor/normal specimens was used to identify somatic coding point mutations, small insertions and deletions, copy number changes and structural events. Tumor RNAseq was used to identify RNA fusions and to perform differential expression analysis. Somatic variant detection, copy number analysis and translocation and RNA fusion detection were performed as previously described.[4] Differential expression analysis was performed using Cuffdiff and DESeq2 and utilizing RNAseq data generated from five separate commercially purchased RNA controls (cerebellum, occipital cortex, brain homogenate, brain stem and fetal brain). A corrected p value of ≤0.05 and a log2 fold change ≥2.0 (tumor expression over control RNA expression) were implemented as thresholds for significant changes. WES was performed for 14 subjects; a 562-gene targeted exome panel (Ashion's Genomic-Enabled Medicine [GEM] Cancer Panel) was performed for one subject, P-05. Additional details on WES and RNAseq analysis are provided in the Supporting Information Methods. Significant expression changes in genes associated with a drug rule were reported to the molecular tumor board.

Specific alterations were matched to potential therapeutics in the study pharmacopeia using a custom set of drug rules and a heuristic approach, as previously described.[4,13] The study pharmacopeia included all oncology drugs in the US Pharmacopeia, as well as select noncancer drugs (herein referred to as repositioned agents). These repositioned agents were included due to emerging evidence suggesting their potential activity in cancer-relevant pathways and clinical experience indicating these agents are well tolerated.[14] Additional details are mentioned in Supporting Information Methods.

Molecular profiling results were presented to a multidisciplinary molecular tumor board as an interpretive genomic report listing specific molecular findings and associated therapeutic associations. The genomics report included all variants triggering a study drug rule. First priority for therapeutic targeting was given to DNA level events (mutations, focal copy number events and structural variants); among those, DNA events with associated RNA variants (i.e., *PDGFRA* amplification and RNA overexpression; DNA mutations also detected at the RNA level) were given the highest priority. Lower priority was given to associations triggered solely due to RNAseq-derived differential expression data (i.e., PDGFRA overexpression). Descriptive information was presented for all reported alterations, including the specific aberration, DNA and RNA allele frequencies (as applicable), expert annotation describing the role for the alteration in DIPG, and curated evidence supporting the association between the alteration and potential therapeutic agents. Pharmacokinetic features related to central nervous system (CNS) penetration and potential CNS activity for the indicated therapies were also included.

Following discussion of the clinical and genomic reports, the specialized tumor board reached a consensus on a treatment recommendation, including dosing and recommended order for combining and introducing the recommended agents. Priority was given to drugs with known pediatric dosing and evidence of adequate CNS penetration. We aimed to target each molecular alteration with the same agent based on an *a priori* set of rules to assess scientific support for a chosen drug and to evaluate clinical feasibility of a drug combination. Additionally, the tumor board prioritized combination strategies for which toxicity data was available. Order of priority for scientific evidence that the agent demonstrated activity against the specific alteration was as follows: (*i*) clinical data was prioritized over preclinical data; (*ii*) preclinical data in relevant models of DIPG was prioritized over data in models that were not DIPG specific, such as high-grade glioma or other brain tumor models. Order of scientific priority was then followed by a feasibility assessment, which included review of any clinical data or published evidence that was available for the proposed drug or drug combination. For most cases, the available information on feasibility of drug combinations was frequently very limited. Therefore, we carefully reviewed side effect profiles of individual drugs to assess feasibility of clinical application and to potentially avoid significant overlapping toxicities. We focused on combination strategies with nonoverlapping toxicities and therefore also integrated repurposing drugs.

WGS and processing

Tumor and constitutional DNA remaining from the original clinical biopsy submission and from recurrence/autopsy when available were subjected to WGS at NantOmics. The WGS cohort also included genomic DNA from three patient-derived cell lines. DNA was randomly fragmented and 100 bp paired-end libraries were constructed. Tumor samples were sequenced at 60× coverage and blood samples sequenced at 30× coverage. Additional details are mentioned in Supporting Information Methods.

Accession to raw genomic data

BAM files are available on Cavatica: https://cavatica.sbgenomics.com/p/datasets#cavatica/cbttc-mixed-pa-01. Cavatica meets the criteria of the National Institutes of Health (NIH) Genomic Data Sharing policies.

Development of patient-derived cell lines

Cell line model development was attempted when feasible.[15] Briefly, biopsy tissues were collected in hibernate A media, mechanically dissociated, followed by red blood cell digestion and expanded in tumor stem media.[16]

CtDNA assessment

ctDNA was collected at baseline as well as with each MRI using standard plasma collection procedures. CtDNA extractions were performed using the QIAamp circulating nucleic acid extraction kit (Qiagen, Germantown, MD). All ctDNA samples were processed for droplet digital PCR and preamplified using forward and reverse primers for *H3F3A* and *HIST1H3B* as previously described.[17] The preamplification as outlined previously is a crucial step for the success of this protocol.[18] Preamplified products were used for analysis of the H3K27M mutation in

Table 1. Patient characteristics, genomic findings and therapy recommendations

Patient ID	Sex	Age at diagnosis, years	Pathology diagnosis	Time from biopsy to start of radiation therapy, days	Analysis overview				Alterations considered for therapy decisions based on WES and RNA sequencing	Therapy recommendation; Followed recommendation (Y/N)	Biopsy at progression	OS (months)
					WES	RNA seq	WGS	ctDNA				
P-01	F	4	Diffuse midline glioma, H3 K27M-mutant, WHO gr IV	9	Yes	Yes	Yes	Yes	TOP2A, YES1	Etoposide, Dasatinib; *N*	No	29.4
P-02	F	5	Diffuse midline glioma, H3 K27M-mutant, WHO gr IV	13	Yes	Yes	Yes	Yes	PDGFRA, KDR, KIT, MET, TOP2A	Mebendazole, Cabozantinib, Etoposide; *Y*	No	5.7
P-04	M	9	Diffuse astrocytoma, IDH- and H3-wildtype, WHO gr II	6	Yes	Yes	Yes	Yes	TP53 A159P	Sertraline; *N*	No	13.2
P-05	M	7	Diffuse midline glioma, H3 K27M-mutant, WHO gr IV	21	Yes	Yes	Yes	Yes	H3F3A K27M, PDGFRA, KDR, KIT	Panobinostat, Mebendazole; *N*	No	13.1
P-06	M	13	Diffuse midline glioma, H3 K27M-mutant, WHO gr IV	14	Yes	Yes	Yes	Yes	H3F3A K27M, PDGFRA	Panobinostat, Mebendazole; *Y*	Yes	23.5
P-07	F	7	Diffuse midline glioma, H3 K27M-mutant, WHO gr IV	13	Yes	Yes	Yes	Yes	H3F3A K27M, PDGFRA, PIK3R1 K567E, TP53 R282W	Panobinostat, Everolimus, Sertraline, Mebendazole; *N*	Yes	8.0
P-08	M	14	Diffuse midline glioma, H3 K27M-mutant, WHO gr IV	14	Yes	Yes	Yes	Yes	H3F3A K27M	Panobinostat; *Y*	No	18.7
P-09	F	7	Diffuse midline glioma, H3 K27M-mutant, WHO gr IV	6	Yes	Yes	Yes	Yes	H3F3A K27M	Panobinostat; *N*	No	23.4
P-10	M	9	Diffuse midline glioma, H3 K27M-mutant, WHO gr IV	13	Yes	Yes	Yes	Yes	H3F3A K27M, BRAF V600E, MAP3K8	Panobinostat, Dabrafenib, Trametinib, Minocycline; *Y*	No	8.1
P-11	M	25	Anaplastic astrocytoma, H3-wildtype, WHO gr II	17	Yes	Yes	Yes	Yes	PDGFRA, TOP2A, IGF1R, ATRX E2279*	Mebendazole, Etoposide, Metformin, Carboplatin; *Y*	No	39.4
P-12	M	10	Diffuse midline glioma, H3 K27M-mutant, WHO gr IV	22	Yes	Yes	Yes	Yes	H3F3A K27M, PTEN, PDGFRA, KDR, KIT, FOSB	Panobinostat, Everolimus, Mebendazole, Valproic acid; *Y*	No	8.7
P-13	M	5	Diffuse midline glioma, H3 K27M-mutant, WHO gr IV	21	Yes	Yes	Yes	Yes	H3F3A K27M, PDGFRA, MET, FOSB	Panobinostat, Mebendazole, Cabozatinib, Valproic acid; *Y*	No	9.1

(Continues)

Table 1. Patient characteristics, genomic findings and therapy recommendations (Continued)

Patient ID	Sex	Age at diagnosis, years	Pathology diagnosis	Time from biopsy to start of radiation therapy, days	Analysis overview				Alterations considered for therapy decisions based on WES and RNA sequencing	Therapy recommendation; Followed recommendation (Y/N)	Biopsy at progression	OS (months)
					WES	RNA seq	WGS	ctDNA				
P-14	F	6	Diffuse midline glioma, H3 K27M-mutant, WHO gr IV	6	Yes	Yes	Yes	Yes	H3F3A K27M, PDGFRA, MET, FOSB	Panobinostat, Mebendazole, Cabozatinib, Valproic acid; *N*	No	13.1
P-16	F	4	Diffuse midline glioma, H3 K27M-mutant, WHO gr IV	12	Yes	Yes	Yes	Yes	HIST1H3B K27M, PDGFRA, FOSB, FOS	Panobinostat, Mebendazole, Propranolol, Valproic acid; *Y*	No	18.4
P-17	M	5	Diffuse midline glioma, H3 K27M-mutant, WHO gr IV	13	Yes	No	No	Yes	H3F3A K27M, DDX11 R167T	Panobinostat, Olaparib, Irinotecan; *N*	No	13.3

plasma ctDNA by droplet digital PCR (ddPCR; RainDance Technologies, Lexington, MA) using previously described sensitivity and specificity criteria.[17]

Statistical design of the clinical trial

The primary aim of this study was to assess the feasibility of providing a treatment recommendation based on WES and RNAseq analyses within 21 business days from obtaining tissue. Feasibility was defined as at least 85% of patients who underwent biopsy being issued a therapy recommendation within the specified timeframe. With the sample size of 15 patients, there was an 82% chance that the lower confidence bound of a one-tailed 90% confidence interval was at least 60% if the true proportion is 85%.

Outcome statistics

Survival outcomes between subjects that did and did not follow treatment recommendations were compared using Kaplan–Meier survival (KMS) analysis with statistical significance calculated by log-rank test. Statistical analyses were performed in Stata SE v14.0 (College Station, TX).

Clinical data collection and safety monitoring

We utilized a centralized Clinical Trial Management System (OnCore®; Madison, WI) to collect clinical data. The University of California San Francisco (UCSF) Cancer Center Data Safety and Monitoring Committee monitored the trial for safety and protocol conduct. Prior to any patient enrollment, each site received appropriate institutional approvals including final approval from the institutional review board for the entirety of the protocol including both the feasibility and therapeutic portions.

Results

Patient characteristics

A total of 17 patients were enrolled of which two were ineligible based on pathology review: diagnoses included pilocytic astrocytoma (negative for $BRAF^{V600E}$ or KIAA1549-BRAF fusion) in one patient and embryonal tumor with multilayered rosettes, C19MC-altered in the second patient. The 15 remaining subjects consisted of six females and nine male patients with a median age of 7 years (range 4–25 years; Table 1). The median time from biopsy to start of radiation was 13 days (range 6–22 days). In this feasibility cohort, a total of nine adverse events were reported to be related to surgery; of these, eight were grade 1 and one patient had worsening of his baseline grade 2 nystagmus to grade 3 that recovered back to baseline within 2 days from the biopsy.

Molecular analysis of primary DIPGs and therapeutic recommendations

The majority of subjects had tumor content of over 90%. Average mean target coverage for tumor WES was 436× (range, 249–599×), and the average number of mapped reads for RNAseq was 228 M (range: 128 M–400 M; Supporting Information Table S1). RNAseq was not completed for one patient

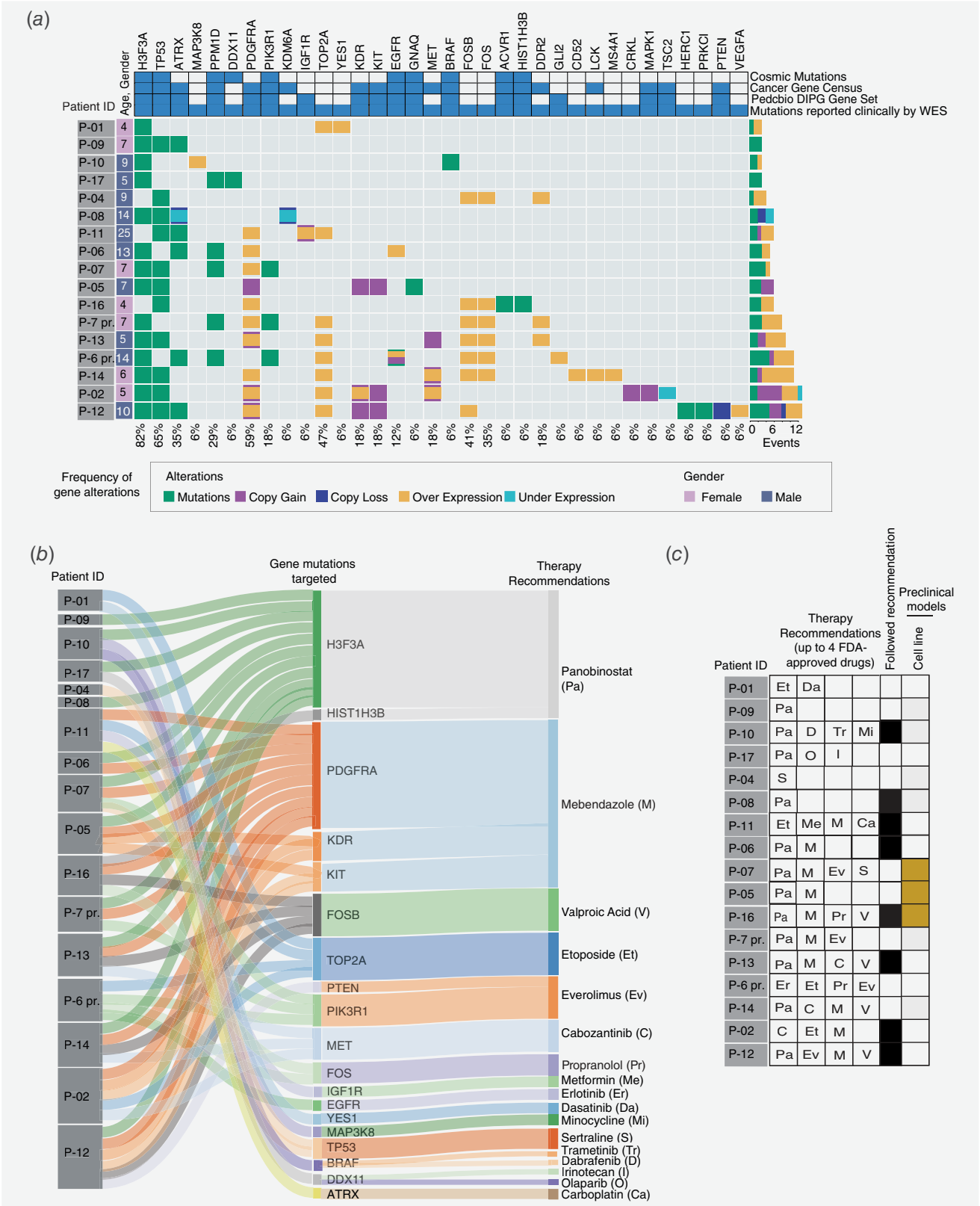

Figure 2. Legend on next page.

due to degraded RNA that failed quality control (QC) RNA integrity number (RIN = 4.8). This was classified as a feasibility failure due to the absence of RNA data for this sample.

WES analysis identified several recurrent genomic alterations across our cohort (Fig. 2*a*, Supporting Information Table S2). The most commonly altered genes were *H3F3A* (n = 12/15; 80%), *TP53* (n = 11/15; 73%), *ATRX* (n = 5/15; 33%), *PDGFRA* (n = 4/15; 27%) and *PPM1D* (n = 3/15; 20%). The most commonly upregulated genes based on RNAseq analysis with potential therapeutic relevance included *PDGFRA* (n = 8/15; 53%), *TOP2A* (n = 6/15; 40%) and *FOSB* (n = 5/15; 33%; Fig. 2*a*).

Treatment recommendations included a variety of FDA approved agents, including targeted oncology agents and repositioned agents (Fig. 2*b* and 2*c*). The histone deacetylase (HDAC) inhibitor, panobinostat, was the most commonly recommended agent (n = 11/15; 73%). Two subjects with H3K27M positive DIPGs (P-01; P-02) were enrolled in the trial prior to the publication reporting potential efficacy of panobinostat in DIPG and as such, panobinostat was not included in their treatment recommendation.[19] Panobinostat was followed in frequency by mebendazole, a repositioned agent. Mebendazole is an antihelmintic agent shown to have inhibitory activity against various kinases including PDGFRA,[20] to display anticancer activity in other tumor types,[21,22] and to have potential CNS activity.[23] Mebendazole was recommended for patients with *PDGFRA* copy number gain (n = 4/15; 27%) as well as for patients whose tumors showed *PDGFRA* overexpression (8/15, 60%), even in the absence of focal copy number gain (Fig. 2*a* and 2*b*). Cabozantinib, a MET inhibitor, was used in three subjects with *MET* amplification, two of which also showed *MET* overexpression. Additional genomic alterations that were used to guide treatment recommendations included a hotspot mutation in *BRAF* (V600E), *IGF1R* amplification and *EGFR* amplification/mutation/overexpression. Valproic acid was recommended in the context of *FOSB* overexpression.[24,25]

Molecular analysis of progressive DIPGs

Within this feasibility study, two subjects underwent a repeat biopsy at time of progression and a second tumor board treatment recommendation was issued based on repeat WES and RNAseq. For P-06, WES found core similarities between initial diagnosis and progression biopsies, including *H3F3A*, *ATRX* and *PPM1D* mutations in both tumor samples. However, WES also revealed additional and potentially therapeutically informative alterations that were only detected in the progression sample, including *EGFR* amplification and $EGFR^{R108K}$ and $PIK3R1^{G376R}$ mutations (Fig. 2*a*). For the second subject (P-07), WES analysis of the sample at progression revealed largely overlapping mutations in the recurrent tumor compared to the primary tumor, including shared mutations in *H3F3A*, *PIK3R1* and *PPM1D*. A subclonal $TP53^{R282W}$ mutation was reported in the primary tumor at a low DNA allele frequency of 5% but did not meet the threshold for clinical reporting in the progressive sample (Fig. 2*a*).

Whole genome sequencing of primary, progressive and autopsy DIPG samples

We performed WGS on longitudinal samples from P-06 and P-07, including primary and progression tumor samples from P-06 and primary, progression and autopsy samples from P-07. As expected, WGS found that gene mutations informing treatment recommendations were retained in both progression samples. WGS analysis further found multiple additional alterations that arose in cancer genes in the progressive tumor (Fig. 3*a*–3*d*; Supporting Information Tables S3 and S4). These results support the concept of likely clonal evolution and/or selection in progressive DIPG tumors.

WGS analysis of P-07 autopsy samples from different regional anatomic locations showed spatial as well as temporal heterogeneity of the tumor (Fig. 3*a* and 3*b*). Circos plot analyses highlight extensive copy number variation in five of the autopsy samples and increased structural variants (SVs) at every autopsy site (Fig. 3*b*).

To inform future molecularly guided clinical trials, we investigated whether WGS provided additional insights into the therapeutic landscape of DIPG. WGS detected all of the coding point mutations reported as potentially clinically actionable by clinical WES (Supporting Information Table S5). Variants detected by WGS were next evaluated using the PNOC003 study pharmacopeia and drug rules. Two additional alterations that triggered drug rules were identified from WGS, specifically $IDH1^{R132H}$ in P-11, which is a well-defined mutation in gliomas being targeted in clinical trials (NCT03343197), and $ATRX^{L563X}$ in P-07. While both alterations were detected by WES, they were outside the reportable range of the clinical WES assay. WGS results are shown as circos plots in Supporting Information Figure S1, with altered gene names, copy number variations (CNVs) and overall number

Figure 2. Overview of alterations based on Whole Exome Sequencing (WES) and RNA sequencing (RNAseq) and assigned therapy recommendations in subjects enrolled in the feasibility portion of PNOC003. (*a*) Oncoprint representation of selected alterations identified *via* WES and RNAseq in primary DIPG tumors from 15 patients and two recurrent tumors. Patients are represented in rows and genes are labeled in columns. Patients with recurrent tumors are labeled with "-pr". Annotations in blue show whether these mutations were identified with cancer relevant mutations in specified databases, and genes frequently involved as the major driver mutations in DIPGs uploaded on PedcBioPortal for Cancer Genomics.[41] Copy gain and loss for indicated genes reflect focal events; whole chromosome gain/loss are not displayed. (*b*) Sankey diagram to represent the individualized, targeted therapy recommendations for each PNOC003 patient based on specific gene alterations identified via molecular profiling. First node shows patient IDs that is connected to the therapeutically informative genes that are mutated in the second node. Third node depicts the targeted therapy agents recommended by the tumor board, abbreviations used for drugs are shown in parentheses. (*c*) Summary of therapeutic options recommended to patients along with patient decision to follow the recommendations (filled boxes) or not (blank boxes).

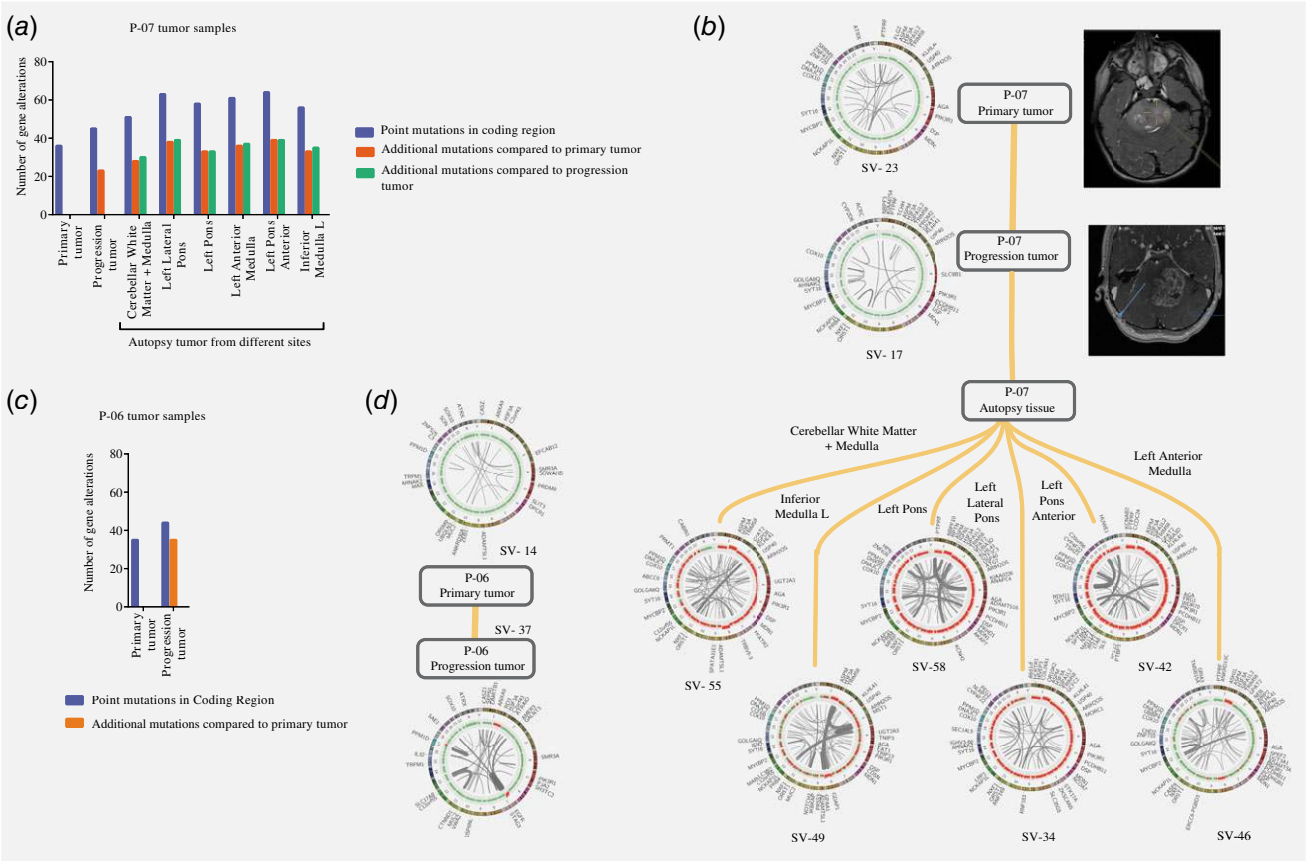

Figure 3. Whole genome sequencing of PNOC003 patient-derived DIPG tumors shows temporal and spatial evolution of DIPG tumors from initial diagnosis, progression and autopsy. (*a*, *c*) Bar graph representing WGS-detected gene mutations (blue bars) in primary DIPG tumor and progression tumor of P-07 and P-06, respectively and tumor from six autopsy sites of P-07. Red bar shows unique mutations found in progression and autopsy samples compared to primary tumor, green shows unique mutations compared to progression tumors. (*b*, *d*) Circos plot representation of the altered genes, CNVs and structural alterations identified in primary DIPG tumor and progression tumor of P-07 and P-06, respectively and tumor from six autopsy sites of P-07. SV, structural variations per patient; Circos plot legend: outermost ring is chromosome number; inner ring is copy number—green is normal, blue is copy loss and red shows copy gain; innermost lines represent SV.

of SVs highlighting the vast genetic heterogeneity across DIPG patients enrolled in this trial (Supporting Information Table S3). Consistent with previous reports, we found a trend between the *TP53* mutation status and total number of SVs found in these DIPGs. Tumors with less than 30 SVs were classified as low SV group and had either *TP53* wild-type (including *PPM1D* mutant) or *TP53* single copy alteration. Conversely, all samples with higher SV counts (>30) were *TP53* mutant, and all but one had evidence for two hits in *TP53* (two mutations, or one mutation with loss of the remaining wild-type allele). This hints at *TP53* mutation as a putative cause of genomic instability and associated structural heterogeneity observed in DIPGs, however, a larger sample set is needed to draw statistically significant conclusions.

DIPG derived preclinical models

WGS was performed to evaluate the fidelity of the cell line model to the matched primary tumor (P-05, P-07 and P-16). Compared to the matched primary tumor, the cell lines retained key recurrent genomic alterations such as mutations in *H3F3A* or *HIST1H3B* as well as in *ACVR1*, *TP53*, *PPM1D* and *PIK3R1*. An *ATRX* deletion reported for P-05 was also detected in the P-05 cell line. However, *PDGFRA*/*KDR*/*KIT* copy number gain detected in this same patient tumor was not seen in the patient-derived cell line despite being maintained as a neurosphere. In addition, the cell lines show additional coding mutations not detected in the primary tumor (Fig. 4, Supporting Information Table S6).

Detection of H3K27M in plasma ctDNA

In adult CNS cancers, ctDNA is used for tumor profiling, facilitating diagnosis and monitoring response to therapy.[26,27] We were able to assess *H3F3A* and *HIST1H3B* wild type and mutant alleles, which allowed for assessing the mutation allele frequency (MAF). MAF above 0.001% was considered as positive detection (Fig. 5*a*). We successfully detected H3K27M mutation at diagnosis in 11/13 (85%) of subjects positive for histone mutation as assessed by biopsy-informed WES (Fig. 5*b*). Our plasma ctDNA analysis further detected circulating mutant histone at postradiation (6/6; 100%), during treatment (7/7; 100%), at progression (5/7; 71%) and at the end of study visit (5/5; 100%; Fig. 5*c*).

(*a*)

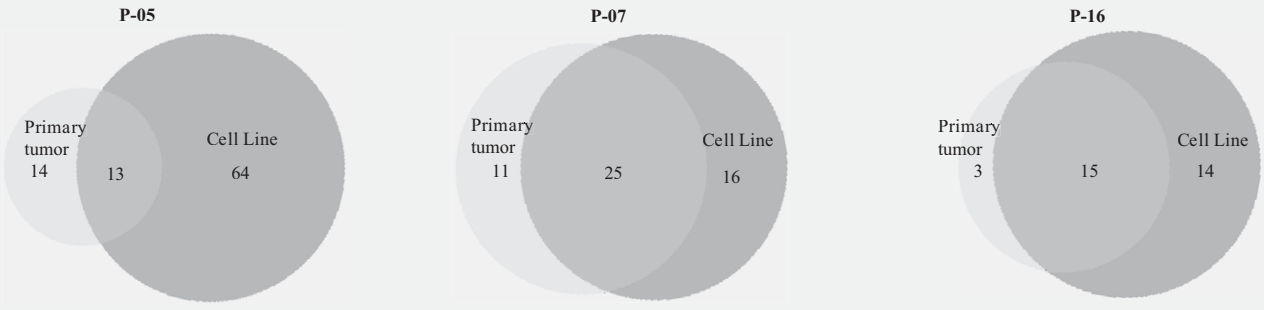

(*b*)

Shared Mutations in P-05 derived cell line	Shared Mutations in P-07 derived cell line	Shared Mutations in P-16 derived cell line
H3F3A (K27M)	H3F3A (K27M)	HIST1H3B (K27M)
TP53 (A159P)	PIK3R1 (K567E)	ACVR1 (R206H)
RAB17 (V83I)	PPM1D (L546P)	TP53 (R248Q)
NDUFB4 (R57L)	MYOM3 (D1210 Silent)	SAMD11 (P628 Silent)
DNAH11 (A3625E)	PTPRF (Splice Site Donor+Intron)	TTN (R11096H)
TAS2R40 (V167E)	ASPM (H2868P)	CBLL1 (P64L)
PRSS3 (L98 Silent)	SIPA1L2 (W1297 Stop Gained)	PDGFRL (P188 Silent)
KDM4E (V212 Silent)	RYR2 (C1912 Silent)	OR5M10 (L115 Silent)
ANO2 (S822 Silent)	TRIM58 (I40T)	OR10W1 (Q78K)
KCNH5 (R504Q)	RP11-724O16.1 (N407S)	NRXN2 (R598Q)
SLC19A1 (P221R)	USP40 (R792 Stop Gained)	PIBF1 (R271 Silent)
CAPN6 (R408C)	DSP (A247V)	FEM1A (E358 Silent)
SOX10 (S419Wfs*22 Frame Shift)	MDN1 (A576V)	TAF4 (S1042 Silent)
	PMS2 (3' UTR)	ARMCX5 (V90 Silent)
	PRUNE2 (L276 Silent)	ACVR1B (Y100* Frame Shift)
	NXF1 (R511 Stop Gained)	
	NCKAP1L (V816I)	
	MYCBP2 (Splice Site Donor+Intron)	
	SYT16 (V413I)	
	CAMTA2 (P772 Silent)	
	COX10 (S415N)	
	ARIH2OS (L106L silent)	
	AGA (L126Ffs*18 Frame Shift)	
	OR5T1 (N101K)	
	DNAJC7 (G432G silent)	

Figure 4. Whole genome sequencing of PNOC003 patient-derived DIPG cell lines shows original and divergent mutations. (*a*) Venn diagram representing WGS-detected gene mutations in the coding region in primary DIPG tumor and derived cell lines for P-05, P-07 and P-16. (*b*) Table of shared mutations retained in primary tumor and derived cell line.

Treatment and clinical outcomes

Eight patients in the feasibility cohort followed the molecular tumor board recommendations, while seven did not. At the time of the data analysis (October 11, 2018), 14/15 had progressed and died of disease. One patient who followed the therapy recommendation remains alive (P-11); however, came off therapy due to progression at 30.8 months from diagnosis and 27.4 months from initiation of on-study therapy. The patient's tumor was H3 wild type and demonstrated the following targetable mutations: $ATRX^{E2279*}$, TOP2A overexpression, PDGFRA overexpression, and IGF1R copy number gain and overexpression. The patient was initially treated with carboplatin to target $ATRX^{E2279*}$; metformin to target IGF1R copy number gain and overexpression; mebendazole to target PDGFRA overexpression (replaced by dasatinib at cycle 3); and etoposide to target TOP2A overexpression. Patients that followed therapy recommendations remained on therapy for a median of 3.8 months from initiation of at least one study drug and a median of 2.9 months from initiation of the combination of study drugs (due to step-wise introduction of drugs over successive cycles). Although the feasibility portion of this study was not designed to determine therapeutic efficacy, the patients that followed treatment recommendations and did not follow treatment recommendations appeared to have similar median overall survival of 13.8 months and 13.2 months, respectively (overall median of 13.2 months; p value = 0.86).

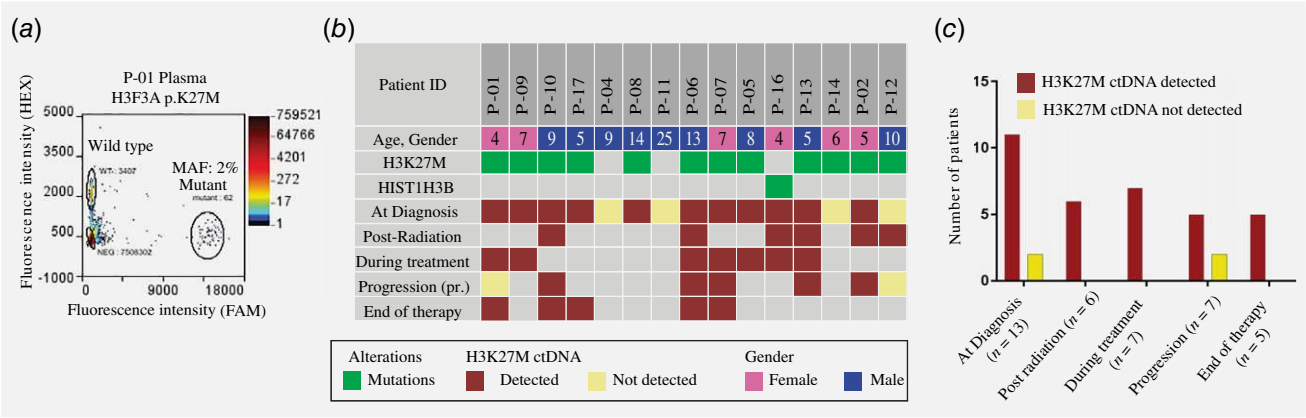

Figure 5. Detection of H3K27M mutant ctDNA in plasma. (*a*) Representative digital droplet PCR (ddPCR) plot of *H3F3A* wild type and H3K27M mutant detection for plasma at initial diagnosis for P-01. (*b*) Serially collected plasma samples analyzed for detection of H3K27M during course of disease. (*c*) H3K27M ctDNA was detected in 85% of patients at diagnosis, 100% at post radiation/during therapy, 71% at progression and in 100% at the end of therapy.

Discussion

We report on the feasibility of implementing a precision medicine approach using next-generation sequencing for subjects with DIPG within a multi-institutional setting. To the best of our knowledge, this is the first trial demonstrating the feasibility of a genomic-based, real-time, multiagent therapy approach for treatment of newly diagnosed patients with DIPG.

Biopsy for radiographically presumed DIPG has been a historically controversial topic; however, during the past 5 years, surgical biopsies in children with DIPG were shown to be performed safely with acceptable risks.[6,7] While these trials demonstrated low mortality and morbidity risk associated with the surgical procedure, the current feasibility trial is the first to apply such biopsies for comprehensive clinical characterization of the mutational and expression landscape of tumors via WES and mRNA expression analyses and to utilize such analyses to inform therapy via a combinatorial targeting approach in real-time. We have shown that this approach is indeed feasible in the majority of patients (14/15; 93%) and that a specialized tumor board can render a comprehensive treatment plan with up to four FDA-approved agents within a clinically relevant timeframe of 21 business days or less. Within our trial, two out of 17 subjects were thought to have DIPG based on imaging but, were found to have alternative diagnoses (pilocytic astrocytoma; embryonal tumor with multilayered rosettes, C19MC-altered). These findings highlight the diagnostic utility of a biopsy approach and suggest that even at highly experienced pediatric neuro-oncology centers, imaging alone can be misleading.

Within our cohort, 80% of subjects' DIPGs harbored oncohistone H3K27M mutations (11/15 *H3F3A* and 1/15 *HIST1H3B*), 73% demonstrated *TP53* mutations, 27% showed *PDGFRA* alterations and 33% of patients displayed alterations in *ATRX*, a previously reported combinatorial mutation pattern in DIPGs.[28] However, no two patients possessed identical mutational landscapes. One patient's DIPG carried a $BRAF^{V600E}$ mutation along with the *H3F3A* mutation. Cooccurrence of these two mutations has now been reported in several pediatric CNS tumors.[29–31] Unfortunately, this patient progressed and died of disease only 8 months from diagnosis. Interestingly, one patient displayed cooccurrence of a *PPM1D* (DNA allele frequency 33%) and *TP53* mutation (5% DNA allele frequency, likely subclonal). Generally, *PPM1D* and *TP53* mutations are mutually exclusive, with a rare exception in one previously reported DIPG exhibiting clonal heterogeneity in *H3.3K27M-TP53* and *H3.3K27M-PPM1D*.[9]

Given the relative paucity of genomic alterations in pediatric tumors,[32] the addition of RNAseq can be useful to guide therapy. The main challenge with RNAseq remains the utilization of appropriate control tissue for differential expression analysis. To address this concern, we used multiple independent control RNAs. However, additional studies are needed to analyze, and integrate RNAseq data for informing future therapeutic strategies with respect to the identity of DIPG cell of origin.

As part of this feasibility trial, we also assessed the practicality of obtaining biopsies at the time of first progression. There is now significant evidence that the molecular profile of DIPGs changes with therapy and in the course of tumor progression and many centers are now consistently obtaining tumor tissue at time of recurrence for a variety of brain tumor diagnoses.[33,34] Within this study, two subjects underwent a repeat biopsy. Interestingly, for one subject (P-06), the recurrent tumor showed activation of the EGFR pathway by a new activating mutation in *EGFR* as well as focal *EGFR* amplification, in addition to a *PIK3R1* mutation. RNAseq analysis further confirmed pathway upregulation. While *EGFR* mutations are rare in pediatric DIPG, mutations in the extracellular ligand binding domain of EGFR including the R108K mutation have been reported in adult glioblastoma.[35,36] It is possible that these new alterations were present in the initial tumor but were not detected at initial diagnosis, potentially due to spatial heterogeneity. Given the eloquent area of these brainstem tumors, we have not embarked on obtaining regional biopsies of

these tumors, limiting our ability to assess spatial heterogeneity at diagnosis. However, the low acceptance rate of families for a repeat biopsy at time of progression makes this approach less attractive to determine potential therapy-related changes within the tumor, and alternative, less invasive approaches are needed.

To this end, we explored the utility of collecting ctDNA to determine if we can reliably detect one of the key driver mutations of DIPG (H3K27M). Previous studies have shown that this specific mutation can be detected in the cerebrospinal fluid (CSF) of children with midline glioma.[37] However, CSF is rarely collected in children with DIPG due to concerns of herniation. Here, we were able to detect the H3K27 mutation in the plasma of 85% of cases at diagnosis and in 100% of cases during therapy. This suggests the feasibility of expanding this platform to assess other driver mutations with the ultimate goal of using ctDNA as a diagnostic and prognostic tool to assess molecular alterations associated with therapy and/or progression.

As part of the study, we were able to establish several patient-derived cell lines. Based on sequencing analysis, these cell lines retain several key genomic alterations that are typical of DIPG, including *H3F3A/HIST1H3B, TP53, PPM1D, ACVR1* and *PIK3R1* mutations. However, cell lines differ from their matched primary tumors, displaying multiple additional alterations that either reflect clonal selection or *de novo* mutations arising during establishing of these lines.[38] These findings highlight potential limitation of such model systems.

To address key decisions and platform implementation challenges associated with clinical next-generation sequencing for pediatric DIPG, we performed WGS analysis retrospectively and compared results to WES. Overall, WGS did not reveal any additional therapeutic recommendations except in patient, P-05. However, WGS studies have increasingly implicated recurrent mutated regulatory sites in cancer and altered enhancer activities due to mutations or structural genomic alterations.[39] Similarly, the importance and prevalence of noncoding RNAs and/or altered RNA processing in regulating cancer biology are being validated across multiple cancers.[40] As such, the combination of epigenetic dysregulation with noncoding mutations and/or altered RNA processes can dramatically alter the actionable therapeutic avenues to be implemented for DIPGs. Based on observed differences in platforms in cancer-relevant targets and to support RNAseq interpretation, we propose that the next generation of DIPG clinical trials should include a more comprehensive platform that includes WES, WGS, RNAseq and potentially a targeted, deep coverage panel.

Although this feasibility study did not mandate patients to follow tumor board recommended precision therapy, we have amended the current protocol to enroll a larger cohort of patients. The reasons that patients and families did not follow treatment recommendations were multifactorial. Some subjects ultimately enrolled in an alternate clinical trial after the biopsy. Other families transitioned to therapy options that focused on quality of life, while others elected to pursue alternative therapies. Unfortunately, the current feasibility cohort did not demonstrate survival benefit of our precision medicine approach; however, this must be considered in the setting of a very small sample size. The feasibility cohort of the trial was not designed to confirm efficacy or to make judgment on the impact of this approach on overall survival. In contrast, the goal of the expansion cohort will be to better clarify the impact of this approach on survival and on the overall clinical outcome of patients with DIPG, with the ultimate goal to better detect differences in outcome of patients that follow recommended therapy *vs.* those who do not.

Acknowledgements

The authors would like to acknowledge the generosity of all patients and their families for participating in this study. We thank all clinical staff at the PNOC sites who cared for these patients. We acknowledge John Carpten and David Craig for having pioneered the implementation pipeline underlying TGEN Genomics-Guided Treatment Practice. We appreciate help from the Brain Tumor Center Tissue Core at UCSF for handling and shipping both clinical trial and autopsy samples. We thank members of the Children's Brain tumor Tissue Consortium (CBTTC) and its operation center including Jennifer Mason, Elizabeth Appert, Mateusz Koptyra, David Stokes and Jena Lilly along with Pichai Raman and Allison Heath from the D3b team. We would also like to thank all members of PNOC for their support. We also thank Mitch Berger, UCSF for his ongoing support of this study and guidance. This work was funded by the V Foundation (Atlanta, GA), Pediatric Brain Tumor Foundation (Asheville, NC), TGEN Foundation, Dragon Master Foundation, Kortney Rose Foundation, Musella Foundation, Project Open DIPG, The Gabriella Miller Kids First Data Resource Center, Goldwin foundation, Smashing Walnuts Foundation, Piedmont Community Foundation, Matthew Larson Foundation, Kaminsky Foundation, the PNOC Foundation, the Jenny's Qust Foundation as well as generous donations from families and patients.

Author Contribution

S.M., M.E.B., J.N., M.P., A.C.R., S.B., W.L. and A.M. performed design and conceptualization of the study; S.M., W.S.L., L.K., N.G., S.N.M., C.K., R.P., S.N., S.A.B., M.E.B., M.P., J.R.C., K.Z., A.B. and J.K. provided clinical trial implementation, data collection and reporting; S.M., P.J., W.S.L., L.K., E.P., B.Z., Y.Z., A.R., S.N., S.A.B., M.E.B., D.S., C.K., A.M., J.K., A.B., J.N. and A.C.R. performed analysis and interpretation of the clinical and genomic data; and S.M., P.J., W.S.L., E.P., B.Z., Y.Z., A.R., S.N., A.J.W., S.A.B., M.E.B., J.N., C.K., M.P., A.C.R., C.K.P., N.T., J.J.P. and D.S. drafted, edited and reviewed the manuscript.

References

1. Cohen KJ, Heideman RL, Zhou T, et al. Temozolomide in the treatment of children with newly diagnosed diffuse intrinsic pontine gliomas: a report from the Children's Oncology Group. *Neuro Oncol* 2011;13:410–6.
2. Jansen MH, van Vuurden DG, Vandertop WP, et al. Diffuse intrinsic pontine gliomas: a systematic update on clinical trials and biology. *Cancer Treat Rev* 2012;38:27–35.
3. Borad MJ, Egan JB, Condjella RM, et al. Clinical implementation of integrated genomic profiling in patients with advanced cancers. *Sci Rep* 2016; 6:25.
4. Byron SA, Tran NL, Halperin RF, et al. Prospective feasibility trial for genomics-informed treatment in recurrent and progressive glioblastoma. *Clin Cancer Res* 2018;24: 295–305.
5. Radovich M, Kiel PJ, Nance SM, et al. Clinical benefit of a precision medicine based approach

for guiding treatment of refractory cancers. *Oncotarget* 2016;7:56491–500.
6. Cage TA, Samagh SP, Mueller S, et al. Feasibility, safety, and indications for surgical biopsy of intrinsic brainstem tumors in children. *Childs Nerv Syst* 2013;29:1313–9.
7. Puget S, Beccaria K, Blauwblomme T, et al. Biopsy in a series of 130 pediatric diffuse intrinsic pontine gliomas. *Childs Nerv Syst* 2015;31:1773–80.
8. Bugiani M, Veldhuijzen van Zanten SEM, Caretti V, et al. Deceptive morphologic and epigenetic heterogeneity in diffuse intrinsic pontine glioma. *Oncotarget* 2017;8:60447–52.
9. Nikbakht H, Panditharatna E, Mikael LG, et al. Spatial and temporal homogeneity of driver mutations in diffuse intrinsic pontine glioma. *Nat Commun* 2016;7:11185.
10. Chan KM, Fang D, Gan H, et al. The histone H3.3K27M mutation in pediatric glioma reprograms H3K27 methylation and gene expression. *Genes Dev* 2013;27:985–90.
11. Gupta N, Goumnerova LC, Manley P, et al. Prospective feasibility and safety assessment of surgical biopsy for patients with newly diagnosed diffuse intrinsic pontine glioma. *Neuro Oncol* 2018;20:1547–55.
12. Kambhampati M, Perez JP, Yadavilli S, et al. A standardized autopsy procurement allows for the comprehensive study of DIPG biology. *Oncotarget* 2015;6:12740–7.
13. Nasser S, Kurdolgu AA, Izatt T, et al. An integrated framework for reporting clinically relevant biomarkers from paired tumor/normal genomic and transcriptomic sequencing data in support of clinical trials in personalized medicine. *Pac Symp Biocomput* 2015;20:56–67.
14. Kast RE, Karpel-Massler G, Halatsch ME. CUSP9* treatment protocol for recurrent glioblastoma: aprepitant, artesunate, auranofin, captopril, celecoxib, disulfiram, itraconazole, ritonavir, sertraline augmenting continuous low dose temozolomide. *Oncotarget* 2014;5:8052–82.
15. Mueller S, Haas-Kogan DA. WEE1 kinase as a target for cancer therapy. *J Clin Oncol* 2015;33:3485–7.
16. Monje M, Mitra SS, Freret ME, et al. Hedgehog-responsive candidate cell of origin for diffuse intrinsic pontine glioma. *Proc Natl Acad Sci USA* 2011;108:4453–8.
17. Panditharatna E, Kilburn LB, Aboian MS, et al. Clinically relevant and minimally invasive tumor surveillance of pediatric diffuse midline gliomas using patient-derived liquid biopsy. *Clin Cancer Res* 2018;24:5850–9.
18. Jackson JB, Choi DS, Luketich JD, et al. Multiplex preamplification of serum DNA to facilitate reliable detection of extremely rare cancer mutations in circulating DNA by digital PCR. *J Mol Diagn* 2016;18:235–43.
19. Grasso CS, Tang Y, Truffaux N, et al. Functionally defined therapeutic targets in diffuse intrinsic pontine glioma. *Nat Med* 2015;21:555–9.
20. Nygren P, Fryknas M, Agerup B, et al. Repositioning of the anthelmintic drug mebendazole for the treatment for colon cancer. *J Cancer Res Clin Oncol* 2013;139:2133–40.
21. Nygren P, Larsson R. Drug repositioning from bench to bedside: tumour remission by the antihelmintic drug mebendazole in refractory metastatic colon cancer. *Acta Oncol* 2014;53:427–8.
22. Bai RY, Staedtke V, Rudin CM, et al. Effective treatment of diverse medulloblastoma models with mebendazole and its impact on tumor angiogenesis. *Neuro Oncol* 2015;17:545–54.
23. Bai RY, Staedtke V, Aprhys CM, et al. Antiparasitic mebendazole shows survival benefit in 2 preclinical models of glioblastoma multiforme. *Neuro Oncol* 2011;13:974–82.
24. Khanim FL, Bradbury CA, Arrazi J, et al. Elevated FOSB-expression; a potential marker of valproate sensitivity in AML. *Br J Haematol* 2009;144:332–41.
25. Felix FH, de Araujo OL, da Trindade KM, et al. Retrospective evaluation of the outcomes of children with diffuse intrinsic pontine glioma treated with radiochemotherapy and valproic acid in a single center. *J Neurooncol* 2014;116:261–6.
26. Pan W, Gu W, Nagpal S, et al. Brain tumor mutations detected in cerebral spinal fluid. *Clin Chem* 2015;61:514–22.
27. De Mattos-Arruda L, Mayor R, Ng CK, et al. Cerebrospinal fluid-derived circulating tumour DNA better represents the genomic alterations of brain tumours than plasma. *Nat Commun* 2015;6:8839.
28. Khuong-Quang DA, Buczkowicz P, Rakopoulos P, et al. K27M mutation in histone H3.3 defines clinically and biologically distinct subgroups of pediatric diffuse intrinsic pontine gliomas. *Acta Neuropathol* 2012;124:439–47.
29. Pages M, Beccaria K, Boddaert N, et al. Co-occurrence of histone H3 K27M and BRAF V600E mutations in paediatric midline grade I ganglioglioma. *Brain Pathol* 2018;28:103–11.
30. Nguyen AT, Colin C, Nanni-Metellus I, et al. Evidence for BRAF V600E and H3F3A K27M double mutations in paediatric glial and glioneuronal tumours. *Neuropathol Appl Neurobiol* 2015;41:403–8.
31. Mistry M, Zhukova N, Merico D, et al. BRAF mutation and CDKN2A deletion define a clinically distinct subgroup of childhood secondary high-grade glioma. *J Clin Oncol* 2015;33:1015–22.
32. Bandopadhayay P, Ramkissoon LA, Jain P, et al. MYB-QKI rearrangements in angiocentric glioma drive tumorigenicity through a tripartite mechanism. *Nat Genet* 2016;48:273–82.
33. Salloum R, DeWire M, Lane A, et al. Patterns of progression in pediatric patients with high-grade glioma or diffuse intrinsic pontine glioma treated with bevacizumab-based therapy at diagnosis. *J Neurooncol* 2015;121:591–8.
34. Verhaak RG, Hoadley KA, Purdom E, et al. Integrated genomic analysis identifies clinically relevant subtypes of glioblastoma characterized by abnormalities in PDGFRA, IDH1, EGFR, and NF1. *Cancer Cell* 2010;17:98–110.
35. Lee J, Kotliarova S, Kotliarov Y, et al. Tumor stem cells derived from glioblastomas cultured in bFGF and EGF more closely mirror the phenotype and genotype of primary tumors than do serum-cultured cell lines. *Cancer Cell* 2006;9:391–403.
36. Brennan CW, Verhaak RG, McKenna A, et al. The somatic genomic landscape of glioblastoma. *Cell* 2013;155:462–77.
37. Huang TY, Piunti A, Lulla RR, et al. Detection of histone H3 mutations in cerebrospinal fluid-derived tumor DNA from children with diffuse midline glioma. *Acta Neuropathol Commun* 2017;5:28.
38. Zhao X, Liu Z, Yu L, et al. Global gene expression profiling confirms the molecular fidelity of primary tumor-based orthotopic xenograft mouse models of medulloblastoma. *Neuro Oncol* 2012;14:574–83.
39. Melton C, Reuter JA, Spacek DV, et al. Recurrent somatic mutations in regulatory regions of human cancer genomes. *Nat Genet* 2015;47:710–6.
40. Sarkies P, Miska EA. Small RNAs break out: the molecular cell biology of mobile small RNAs. *Nat Rev Mol Cell Biol* 2014;15:525–35.
41. Mackay A, Burford A, Carvalho D, et al. Integrated molecular meta-analysis of 1,000 pediatric high-grade and diffuse intrinsic pontine glioma. *Cancer Cell* 2017;32:520–37.